

Free Radical Scavenging Activity of Ultrashort Single-Walled Carbon Nanotubes with Different Structures through Electron Transfer Reactions

Ana Martínez*[†] and Annia Galano*[‡]

Departamento de Materia Condensada y Criogenia, Instituto de Investigaciones en Materiales, Universidad Nacional Autónoma de México, Circuito Exterior S. N., Ciudad Universitaria, CP 04510, México DF, México, and Departamento de Química, División de Ciencias Básicas e Ingeniería, Universidad Autónoma Metropolitana-Iztapalapa, San Rafael Atlixco 186, Col. Vicentina, Iztapalapa, AP POSTAL 55-534, México DF 09340, México

Received: January 7, 2010; Revised Manuscript Received: March 24, 2010

The scavenging activity of ultrashort single-walled carbon nanotubes (US-SWCNTs) is analyzed in this work considering the electron transfer mechanism. Such processes have been modeled using density functional theory for a wide variety of US-SWCNTs and free radicals. Different structures with diverse diameters and helicities (*armchair* and *zigzag*) have been considered. In addition, US-SWCNTs with three different kinds of defects and carboxylic functionalized US-SWCNTs have been taken into account. It stands out that ultrashort *zigzag* nanotubes are better electron acceptors and also slightly better electron donors than their corresponding *armchair* partners. Pristine *zigzag* nanotubes were found to be better electron donors and worse electron acceptors than carboxylated US-SWCNTs. The electron donor capability of carboxylated *armchair* nanotubes is equivalent to that of the pristine US-SWCNT, while they are better electron acceptors than the nonfunctionalized tubes. Our results indicate that neither the length nor the defects have a significant effect on the free radical scavenger capacity of the US-SWCNTs, when reacting through the electron transfer mechanism. The electron transfer reaction mechanism depends on the characteristics of the free radical and on the nature of the nanotubes.

Introduction

Carbon nanotubes (CNTs) have attracted the interest of the scientific community in the last few decades in a very exceptional way. The amount of research focused on them has increased exponentially since the report of Iijima in 1991.¹ The interest in CNTs is very well justified by their remarkable mechanical and electrical properties,^{2–4} which arise from their unique structures and make them ideal candidates for diverse nanotechnological applications. The chemistry of CNTs is equally fascinating. They constitute large arrays of conjugated double bonds, and therefore, they are expected to show great electron donor and acceptor capabilities; i.e., these structures can easily cope with lack or excess of electrons. This particular feature makes them particularly reactive toward free radicals, and has been used to overcome the lack of solubility of CNTs through side wall covalent fictionalization.^{5–13}

Another logical application to the high reactivity of CNTs toward free radicals is to use them as free radical scavengers. This would be a very useful application, since free radicals are known to be highly damaging species to human health and environment. However, this promising area of research is still in its initial stage and much more work should be devoted to it before practical applications can be implemented.¹⁴ So far, there are only five reports^{15–19} looking into the free radical scavenging activity (or antioxidant activity) of carbon nanotubes. Watts et al.¹⁵ were the first to report that multiwalled carbon nanotubes (MWCNTs) and boron-doped CNTs (BCNTs), with a boron

content of ~1%, can act as antioxidants. They found that the oxidation of polystyrene, polyethylene, polypropylene, and poly(vinylidene fluoride) is retarded by the presence of carbon nanotubes. Three years later, Fenoglio et al.¹⁶ tested the scavenging activity of MWCNTs for hydroxyl and superoxide anion radicals and reported that MWCNTs exhibit a remarkable radical scavenging capacity. After these two experimental works, a theoretical investigation on this subject was performed.¹⁷ The reactions of a (5,5) single-walled carbon nanotube (SWCNT) fragment with six different free radicals were modeled, and it was concluded that SWCNTs can act as free radical sponges based on thermodynamic and kinetic considerations. Shortly after, Lucente-Schultz et al.¹⁸ reported new experimental research on the antioxidant ability of SWCNTs. Their results demonstrated the theoretical prediction that pristine SWCNTs are powerful antioxidants. Very recently, another theoretical work dealing with the influence of length, diameter, and helicity of SWCNTs on the free radical scavenging activity of SWCNTs has been reported.¹⁹ In this study, it was proposed that thin and *zigzag* nanotubes are expected to have the best antiradical activity, regardless of their length.

So far, the free radical scavenging activity of SWCNTs has been modeled for a mechanism involving the addition of the free radicals to the walls of the tubes, but the electron transfer mechanism (ET) has not been studied yet. Since ultrashort single-walled carbon nanotubes (US-SWCNTs) were reported before as likely useful for biological and materials applications,²⁰ then it is the main goal of the present work to test if US-SWCNTs with different structures scavenge free radicals through the ET mechanism. It was previously reported that, in order to scavenge free radicals, substances can either donate or accept electrons.²¹ For this reason, the two possible directions

* Authors to whom correspondence should be addressed. E-mail: agalano@prodigy.net.mx (A.G.); martina@iim.unam.mx (A.M.).

[†] Universidad Nacional Autónoma de México.

[‡] Universidad Autónoma Metropolitana-Iztapalapa.

for ET that must be taken into account are (I) from US-SWCNTs to free radicals (FR) and (II) from FRs to SWCNTs:



Such processes have been modeled using density functional theory for a wide variety of US-SWCNTs and free radicals.

Computational Details

Electronic structure calculations have been performed with the Gaussian 03²² package of programs. Full geometry optimizations and frequency calculations were carried out for all of the stationary points using the B3LYP density functional and the 3-21G basis set. No symmetry constraints have been imposed in the geometry optimizations, and a scaling factor of 0.9627 was used for the frequency calculations, as recommended by Irikura et al.²³ The results obtained at this level of theory (B3LYP/3-21G) were validated in a previous work²⁴ by comparison with other calculations at higher levels of theory. The effect of increasing the basis set to 6-31+G(d) on the energetics was found to be less than or about 0.5 kcal/mol. The energies of all of the stationary points were improved by single point calculations at the B3LYP/6-311+G(d) level of theory. Thermodynamic corrections at 298 K were included in the calculation of relative energies. Spin-restricted calculations were used for closed shell systems and unrestricted ones for open shell systems. Local minima were identified by the number of imaginary frequencies (NIMAG = 0). It seems worthwhile to emphasize the fact that any theoretical model aiming to make predictions concerning practical applications must be analyzed in terms of Gibbs energies, which implies the necessity of performing frequency calculations that for the studied systems are particularly expensive. Accordingly, it seems a better compromise to perform frequency calculations at a low level of theory than increase the level and analyze the results only in terms of electronic energy.

The stationary points were first modeled in the gas phase (vacuum), and solvent effects were included *a posteriori* by single point calculations using a polarizable continuum model, specifically the integral-equation formalism (IEF-PCM)²⁵ at the B3LYP/6-311+G(d) level of theory, with benzene and water as solvents for mimicking nonpolar and polar environments, respectively. Polar environments were considered only for functionalized US-SWCNTs, since the other tubes are not expected to be soluble in such media.

A graphical strategy allowing rapid evaluation of full electron transfer processes has been recently proposed.²⁶ It is known as the full electron donor acceptor map (FEDAM) and is a straightforward way of analyzing the relative feasibility to donate, or accept, charge. It is based on vertical ionization energies (VIE) and vertical electron affinities (VEA), and it was thought to facilitate comparisons among antioxidant and anti-reductant substances. Therefore, relative electron acceptance (REA) and electron donation (RIE) indexes were defined with respect to those of F and Na atoms (obtained at the same level of theory) according to the following equations:

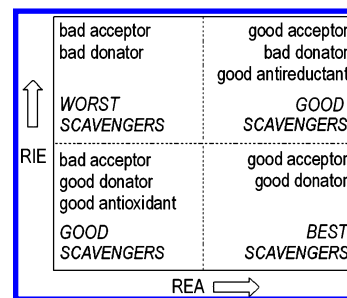


Figure 1. Full electron donor acceptor map (FEDAM).

$$\text{RIE} = \frac{\text{VIE}_L}{\text{VIE}_{\text{Na}}} \quad (1)$$

$$\text{REA} = \frac{\text{VEA}_L}{\text{VEA}_F} \quad (2)$$

where L represents the considered molecule, F represents a good electron acceptor, and Na represents a good electron donor. If RIE is equal to 1, L is as good an electron donor as Na. If RIE > 1, then L is a better electron donor than Na. If RIE < 1, L is a worse electron donor than Na. In the same way, if REA = 1, then L is as good an electron acceptor as F. If REA > 1, then L is a worse electron acceptor than F, and if REA < 1, then L is a better electron acceptor than F.

The FEDAM is then constructed as a plot of RIE versus REA values (Figure 1). In the present work, we will use the corresponding FEDAM to analyze the electron transfer mechanism between US-SWCNTs and free radicals.

Results and Discussion

SWCNTs are cylindrical molecules composed of carbon atoms that can be thought of as rolled-up graphene sheets. Their structures (diameter and helicity) can be unambiguously defined by a chiral vector that represents the roll up direction:

$$C_h = (n, m) = na_1 + ma_2 \quad (3)$$

where a_1 and a_2 denote equivalent lattice vectors of the graphene sheet and n and m are integers ($0 \leq |m| \leq n$). However, it is known that their production does not yield only one kind of well-defined molecules. On the contrary, SWCNTs preferentially aggregate into bundles of different characteristics. These mixtures of SWCNTs widely vary in length, diameter, helicity, and kind, location, and number of defects.^{27–29} Actually producing SWCNTs of defined structures is a major technological challenge.^{30,31} Therefore, it is important to estimate the influence of the above-mentioned structural features on the free radical scavenging activity of SWCNTs.

Accordingly, finite US-SWCNT fragments of extreme helicity (*armchair* and *zigzag*) with diameters ranging from 0.4 to 1.1 nm have been selected for the present study. The tubes have been chosen in such a way that in every case there is an *armchair* and a *zigzag* fragment of similar diameter. The dangling bonds at the ends of the nanotubes have been saturated by hydrogen atoms to avoid unwanted distortions. The thinnest tubes were selected with diameters of ~0.4 nm, since it is the smallest experimentally achievable diameter.³² Different lengths ranging from 0.7 to 2.0 nm (from three to eight hexagons long) have also been tested for the thinnest tubes: (3,3) and (5,0). In addition, US-SWCNTs with different defects have also been

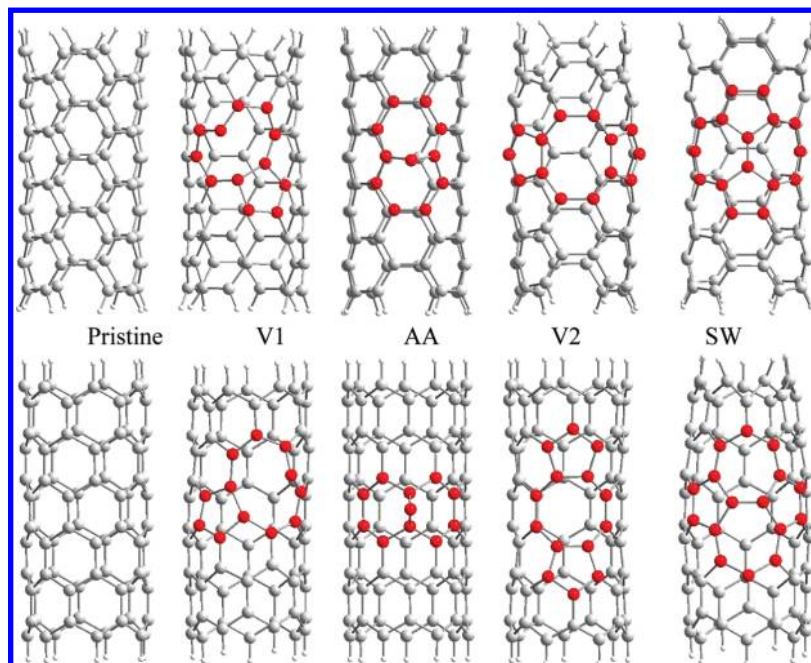


Figure 2. SWCNTs with different defects: vacancies (V), add-atom (AA), and Stone–Wale (SW) defects. Red color is used to aid visualization and indicates the atoms that participate in the defects.

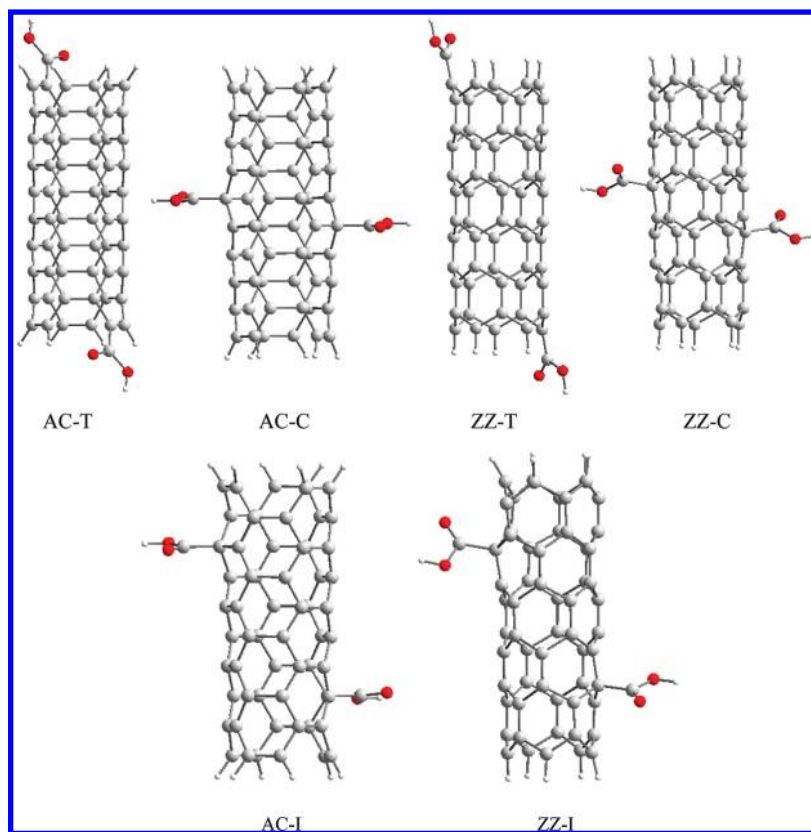


Figure 3. SWCNTs functionalized with –COOH groups. AC-T = *armchair* terminal functionalized, AC-C = *armchair* central functionalized, ZZ-T = *zigzag* terminal functionalized, ZZ-C = *zigzag* central functionalized, AC-I = *armchair* functionalized at an intermediate site (not terminal, not central), and ZZ-I = *zigzag* functionalized at an intermediate site.

studied (Figure 2). Three different kinds of defects have been taken into account: vacancies (V), add-atom (AA), and Stone–Wale (SW) defects. Carboxylic functionalized US-SWCNTs (Figure 3) have also been considered in the present study. They arise from purification,²⁸ are involved in functionalization processes,³³ and have improved solubility in polar solvents.³⁴ There are many other possible configurations than

those included in Figure 3. There are other relative positions of the –COOH groups, and it is also possible to add more than two functional groups. The effect of the number and positions of the functionalization groups added to the US-SWCNTs on its electron donor–acceptor properties might deserve further study. However, such an influence is expected to be proportional to that described in the present study.

TABLE 1: Studied Free Radicals

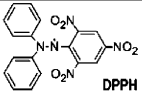
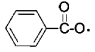
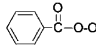
Name	Structure	Name	Structure
R1		R11	$\text{H}_3\text{C}-\text{CH}(\text{O}\cdot)-\text{O}\cdot$
R2	$\cdot\text{O}-\text{H}$	R12	$\text{H}_3\text{C}-\text{C}(\text{CH}_3)(\text{O}\cdot)-\text{O}\cdot$
R3	$\cdot\text{O}-\text{CH}_2-\text{CH}=\text{CH}_2$	R13	$\cdot\text{O}-\text{O}-\text{CH}_2-\text{CH}=\text{CH}_2$
R4	$\cdot\text{O}-\text{CH}_2-\text{CH}=\text{CH}-\text{CH}=\text{CH}_2$	R14	$\cdot\text{O}-\text{O}-\text{CH}_2-\text{CH}=\text{CH}-\text{CH}=\text{CH}_2$
R5	$\text{CH}_2=\text{CH}-\text{CH}(\text{O}\cdot)-\text{CH}=\text{CH}_2$	R15	$\text{CH}_2=\text{CH}-\text{CH}(\text{O}\cdot)-\text{CH}=\text{CH}_2$
R6	$\text{H}_3\text{C}-\text{C}(\text{O}\cdot)-\text{O}\cdot$	R16	$\text{H}_3\text{C}-\text{C}(\text{O}\cdot)-\text{O}\cdot$
R7		R17	
R8	$\cdot\text{O}-\text{O}-\text{H}$	R18	$\cdot\text{O}-\text{O}-\text{CCl}_3$
R9	$\cdot\text{O}-\text{O}-\text{CH}_3$	R19	$\cdot\text{CH}_3$
R10	$\cdot\text{O}-\text{O}-\text{CH}_2-\text{CH}_3$	R20	$\text{O}_2\cdot$

TABLE 2: Diameters (nm) of the Studied Nanotubes

zigzag		armchair	
tube	diameter	tube	diameter
(5,0)	0.392	(3,3)	0.407
(7,0)	0.548	(4,4)	0.542
(9,0)	0.705	(5,5)	0.678
(10,0)	0.783	(6,6)	0.814
(12,0)	0.940	(7,7)	0.949
(14,0)	1.096	(8,8)	1.085

The free radical scavenging activity of the US-SWCNTs has been modeled through the reaction of the above-mentioned fragments with a large set of free radicals (Table 1). These reactions have been computed in the gas phase as well as in benzene or water solutions, aiming for environmental and biological applications, respectively.

In order to avoid mixing the effects of different structural features on the antioxidant activity of US-SWCNTs, the analyses have been performed separately for different subsets of nanotubes. For studying the effect of the helicity, tubes with similar diameter but different helicity were selected (Table 2). Figure 4 shows the corresponding FEDAM in benzene solution. Polar environments have not been considered in this case, since nonfunctionalized US-SWCNTs are not soluble in such media. It stands out that zigzag nanotubes are better electron acceptors and also slightly better electron donors than their corresponding armchair partners. It should be noticed, however, that our models correspond to ultrashort SCNTs, where the condition

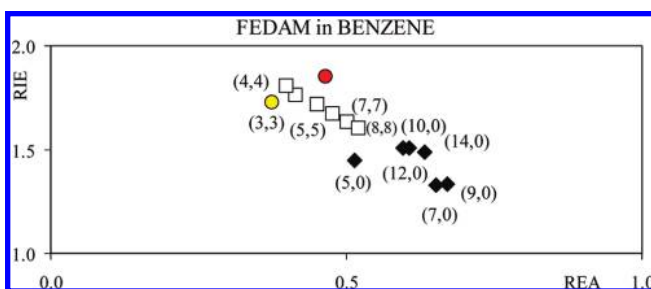


Figure 4. FEDAM in benzene for the pristine nanotubes reported in Table 2. Dots are the corresponding values for carotenoids that were previously reported²⁶ and are included here for comparison (red for astaxanthin (ASTA) and yellow for β -carotene (BC)).

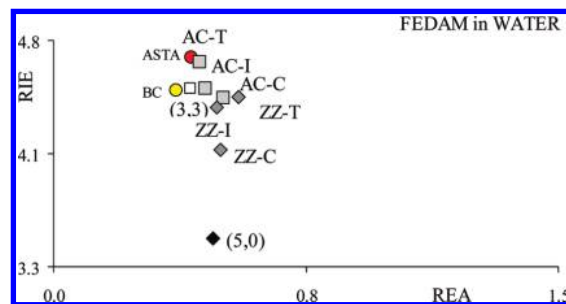


Figure 5. FEDAM in water for different nanotubes. Functionalized nanotubes are shown in Figure 3, and are expected to be soluble in water. ASTA and BC are included for comparison.

$\text{diameter} \ll \text{length}$ does not apply, and therefore there is a gap around the Fermi level.¹⁷ Even though no direct correlation between diameter and the electron acceptor–donor capacity was found, in general, the larger the diameter of the nanotubes, the lower their acceptor–donor capability.

Figure 4 includes the values previously reported²⁶ for two carotenoids. They have been included for comparison purposes, since carotenoids are very well-known for their antioxidant capacity. As the figure shows, zigzag nanotubes are better electron acceptors than carotenoids and also better electron donors. This is also the case for the larger armchair nanotubes: (6,6), (7,7), and (8,8). In fact, β -carotene is the worst electron acceptor and astaxanthin the worst electron donor of all of the compounds in Figure 4. Therefore, regarding the electron transfer mechanism, nanotubes appear to be better to scavenge free radicals than carotenoids.

The effect of functionalization on the electron donor–acceptor capacity of nanotubes has been studied for carboxylated US-SWCNTs (Figure 3). Since they are expected to be soluble in water, the electron donor–acceptor indexes used to build the FEDAM are those corresponding to water solution. For comparison purposes, RIE and REA for nonfunctionalized fragments of similar helicity and diameter were also computed in water, and they were included in the FEDAM as a reference. As Figure 5 shows, $-\text{COOH}$ functional groups significantly modify the electron donor capabilities of US-SWCNTs. Pristine zigzag nanotubes were found to be better electron donors and slightly worse electron acceptors than carboxylated US-SWCNTs. On the other hand, the electron donor capability of carboxylated armchair nanotubes is equivalent to that of the pristine US-SWCNT (with the exception of AC-T), while they are better electron acceptors than the nonfunctionalized tubes. The site of functionalization seems to have only a minor effect, which varies depending on the helicity of the tubes. The studied zigzag fragment, that is carboxylated at the end of the tube (ZZT), shows better electron accepting capability than the corresponding pristine and central (AC-C) functionalized US-SWCNTs. For the armchair fragment, on the other hand, the central carboxylated tube shows the better electron accepting capability. Regarding the electron donor capability, it is slightly higher for centrally functionalized fragments than for those functionalized at terminal or intermediate sites, for both armchair and zigzag configurations.

Comparing Figures 4 and 5, it is possible to see that all of the studied species are better electron donors (RIE is smaller) in benzene than in water, while their electron accepting power is more or less the same in both environments (water and benzene). However, the electron donor–acceptor capability of the US-SWCNTs alone is not enough to make confident predictions. As previously shown for other free radical scav-

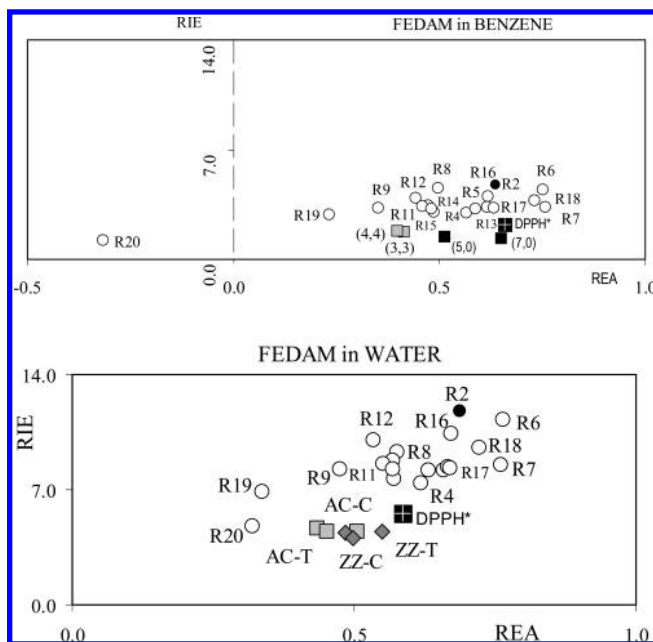


Figure 6. FEDAM in benzene and water for different nanotubes and several free radicals. Please note the scale. The difference between the RIE values is larger than the difference between the REA values.

engers, to properly analyze free radical scavenging processes through ET mechanisms, it is necessary to compare the electron donor–acceptor properties of the scavenger with those of the involved free radicals.²⁶ For the evaluation of the free radical scavenger capacity throughout the ET reaction, we selected the carboxylated nanotubes (soluble in water, better for charge transfer) and four pristine nanotubes. US-SWCNTs (3,3) and (5,0) were selected because they are the thinnest tubes and (4,4) and (7,0) because they are the worse and the best electron donors, respectively.

Figure 6 shows the FEDAM in benzene and water for the selected nanotubes as well as for several free radicals, including the most important for biological systems, i.e., hydroxyl ($\cdot\text{OH}$), peroxy ($\text{ROO}\cdot$), and alkoxy radicals ($\text{RO}\cdot$) (Table 1). 2,2-Diphenyl-1-picryl-hydrazyl (DPPH \cdot) is also incorporated, since it is frequently used to test the free radical scavenging activity in experimental research. The FEDAM facilitates the analysis of the relative acceptor and donor abilities of each free radical–nanotube pair. If nanotubes have lower RIE than free radicals, this means that nanotubes will be better electron donors, while, if they have lower REA, then they are worse electron acceptors than free radicals. As a result, nanotubes will donate an electron to the free radicals and could not accept an electron from the free radicals. In summary, molecules that are located in the upper right section of the map will remove electrons from molecules located in the lower left section of the map. Therefore, the map allows us to predict if the electron transfer process would be feasible, and also helps us to determine which system will be the electron donor and which one the electron acceptor. In general, the electron donor–acceptor properties of free radicals in benzene were found to be closer to those of the nanotubes than they are in water.

It is clear from Figure 6 that free radicals have higher RIEs than the studied nanotubes, meaning that nanotubes are better electron donors than free radicals. However, in benzene, not all free radicals are located rightward to the nanotubes. This indicates that they are not very good electron acceptors with respect to the nanotubes, and in this situation, it is not evident if the ET process will be feasible. FEDAM in water shows that

there are several free radicals located in the upper right section of the map with respect to the nanotubes. Accordingly, for these free radicals, the electron transfer process could take place from the nanotubes to the free radicals. On the contrary, $\text{O}_2^{\cdot-}$ is a better electron acceptor than nanotubes and as good an electron donor as the nanotubes, both in water and in benzene solution. Since nanotubes are not in the upper right section of the map with respect to $\text{O}_2^{\cdot-}$, it cannot be decided if an electron transfer from $\text{O}_2^{\cdot-}$ to the nanotubes is likely to occur. The electron transfer mechanism that is expected to prevail for nanotubes located in the lower left section of the map, when scavenging free radicals (R) located in the upper right section of the map, corresponds to path I. For free radicals that are worse electron acceptors than nanotubes, radical scavengers might act as electron acceptors, according to path II. However, it should be noticed that such a process would be viable only if the free radicals are good electron donors with respect to the nanotubes. Both mechanisms are feasible for the electron transfer process, and the reaction depends on the characteristics of the free radical and on the nature of the nanotubes.

In order to analyze in more detail this process, the energy evolution associated with the electron transfer reactions between US-SWCNT and free radicals has been studied using the corresponding adiabatic Gibbs energy at 298 K. The frequency analysis that is needed to obtain the Gibbs energy is highly computationally expensive, and for this reason, a subset of US-SWCNTs has been selected for this analysis. The four thinnest pristine nanotubes, two *armchair* and two *zigzag*, have been chosen for modeling reactivity in nonpolar environments, and the two thinnest centrally carboxylated tubes have been chosen for the modeling in polar environments.

The adiabatic Gibbs energies of reaction, for paths I and II, are calculated as

$$\Delta G_{\text{ET(I)}}^0 = G_{\text{SWCNT}^{+}} + G_{\text{R}^-} - G_{\text{SCNT}} - G_{\text{R}} \quad (4)$$

$$\Delta G_{\text{ET(II)}}^0 = G_{\text{SWCNT}^{-}} + G_{\text{R}^+} - G_{\text{SCNT}} - G_{\text{R}} \quad (5)$$

The computed values of the adiabatic Gibbs energies reaction, for both paths, are reported in Tables 3 and 4, for benzene and water solutions, respectively. It is important to note that we do not report values for the alkoxy radicals ($\text{RO}\cdot$) reacting with the nanotubes through path II. This is because the optimization of the correspondent cations results in the dissociation of the molecule. The structure of the alkoxy cations is not preserved, and for this reason, it is not possible to analyze this ET reaction. As the values in Table 3 show, in benzene solution, the reactions with most of the free radicals under study are endergonic, regardless of the direction of the ET, in agreement with the predictions from the FEDAM. Path I is exergonic in benzene only for *zigzag* nanotubes and some free radicals. This can be explained by the electron donor capacity of (5,0) and (7,0), which are better electron donors than the *armchair* nanotubes. The most negative values correspond to those free radicals located in the right part of the map. The reaction between (3,3) and (4,4) and the free radicals is exergonic. These nanotubes are the worst electron donors, and apparently, their electron donor power is not enough for the electron transfer reactions with the studied radicals. It is important to mention that the FEDAM allows us to predict which molecule could be the electron donor and which one the electron acceptor. However, the relative position in the FEDAM is not a sufficient condition for the reaction to be exergonic because a significant separation

TABLE 3: Adiabatic Gibbs Energy (kJ/mol), at 298.15 K, for Reactions I and II between Radicals and Radical Scavengers, in Benzene

free radicals	in benzene							
	nanotubes + R [*] → nanotubes ⁺⁺ + R ⁻				nanotubes + R [*] → nanotubes ^{*-} + R ⁺			
	(3,3)	(4,4)	(5,0)	(7,0)	(3,3)	(4,4)	(5,0)	(7,0)
R1	94.7	120.8	21.2	-27.5	331.1	350.7	320.3	181.6
R2	82.0	108.1	8.5	-40.2				
R3	129.4	155.5	55.9	7.2				
R4	159.7	185.8	86.2	37.5				
R5	138.1	164.2	64.6	15.9				
R6	29.3	55.4	-44.2	-92.9				
R7	18.3	44.4	-55.2	-103.9				
R8	196.5	222.6	123.0	74.3	734.1	753.7	723.4	585.6
R9	207.9	234.0	134.4	85.7	664.6	684.2	653.9	515.1
R10	205.3	231.4	131.8	83.1	629.0	648.6	618.2	479.5
R11	225.5	251.6	152.1	103.4	603.9	623.5	593.1	454.4
R12	241.7	267.8	168.2	119.5	579.5	599.1	568.8	430.0
R13	138.0	164.1	64.5	15.8	535.9	555.5	525.1	386.4
R14	207.2	233.3	133.7	85.0	525.9	545.6	515.2	376.4
R15	222.9	249.0	149.4	100.7	533.6	553.3	522.9	384.1
R16	105.2	131.3	31.7	-17.0	587.1	606.7	576.3	437.6
R17	103.0	129.1	29.6	-19.2	550.0	569.6	539.3	400.5
R18	69.9	96.0	-3.6	-52.3	639.7	659.3	629.0	490.2
R19	333.9	360.0	260.4	211.7	543.6	563.2	532.8	394.1
R20	641.9	668.0	568.5	519.7	-12.5	7.1	-23.3	-162.1

TABLE 4: Adiabatic Gibbs Energy (kJ/mol), at 298.15 K, for Reactions I and II between Radicals and Radical Scavengers, in Water

free radicals	in water			
	nanotubes + R [*] → nanotubes ⁺⁺ + R ⁻		nanotubes + R [*] → nanotubes ^{*-} + R ⁺	
	AC-C	ZZ-C	AC-C	ZZ-C
R1	-10.6	-31.94	142.66	144.54
R2	-111.4	-132.72		
R3	-45.2	-66.54		
R4	-8.2	-29.50		
R5	-33.3	-54.61		
R6	-142.0	-163.36		
R7	-143.4	-164.77		
R8	9.4	-11.92		
R9	18.5	-2.86	442.68	444.55
R10	14.3	-7.07	411.50	413.38
R11	42.1	20.72	392.74	394.62
R12	63.3	41.96	376.64	378.51
R13	-49.8	-71.12	319.62	321.50
R14	35.4	14.01	317.30	319.17
R15	46.9	25.59	327.86	329.74
R16	-76.7	-98.06	368.69	370.57
R17	-73.5	-94.83	349.34	351.22
R18	-82.1	-103.42	420.91	422.79
R19	169.2	147.86	308.46	310.34
R20	192.5	171.19	10.70	12.57

between the values is also needed. To analyze if the reaction is feasible, it is necessary to obtain the Gibbs energy or the energetic index (ΔE), as we will see later. Path II was found to be exergonic for all of the reactions involving $O_2^{\cdot-}$, and modeled in benzene. The only exception is the $O_2^{\cdot-}$ reaction with the US-SWCNT (4,4) which is the worst electron acceptor of the studied set. $O_2^{\cdot-}$ is the only free radical able to donate an electron to the nanotubes, and it has been previously proposed to react through path II with other free radical scavengers.³⁵

The results for a polar environment reported in Table 4 show that the number of exergonic processes is significantly increased compared to those taking place in nonpolar media. This is in agreement with the FEDAM; i.e., the reaction is exergonic mainly for those free radicals that are in the upper right section of the map. Comparing among the computed nanotubes, the electron transfer reactions with the *zigzag* US-SWCNTs (ZZ-

C) are more exergonic than the corresponding reactions for the *armchair* nanotube (AC-C). This is also in agreement with the FEDAM, since ZZ-C is a better electron donor than AC-C. In all cases, the reaction is more exergonic for the free radicals that are located in the FEDAM rightward to the nanotubes.

It is important to note that, in water, path II is endergonic for all of the free radicals. In the FEDAM, there are not free radicals with better electron donor capacity than the nanotubes and, for this reason, there will not be an electron transfer from the free radical to the nanotubes in water solution. As demonstrated before, ET in that direction (path II) is favored in nonpolar media for $O_2^{\cdot-}$,³⁵ which is also the only radical able to react as an electron donor with the nanotubes.

The ET reactions can be rationalized within the chemical reactivity theory.²⁶ In view of the fact that electron transfer reactions are favored when the difference between the reactants'

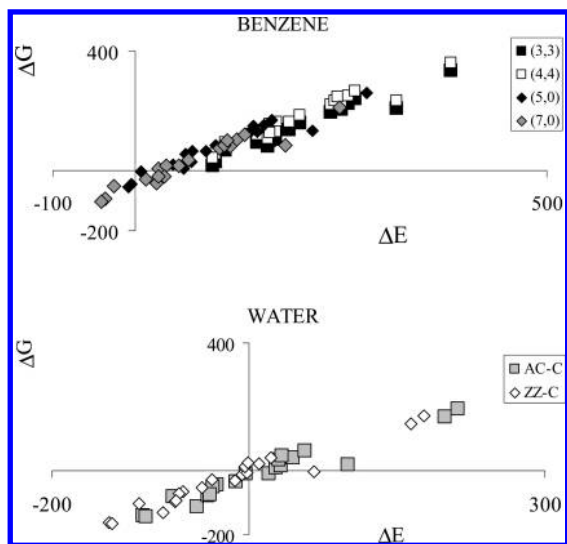


Figure 7. ΔG (in kJ/mol) at 298 K for path I in benzene and water, as a function of ΔE (in kJ/mol) (values are provided as Supporting Information, Tables 1S and 2S).

electronegativities ($\Delta\chi$) is large, and considering that hardness (η) measures the resistance to the flow of electrons, it seems logical to assume that both indexes will affect the electron transfer process. In this context, the energetic index that measures the full electron transfer process is the electronegativity difference plus the arithmetic mean of the hardness:

$$\Delta E = \chi_d - \chi_a + \frac{1}{2}(\eta_d + \eta_a) \quad (6)$$

The electronegativity of each species is calculated as

$$\chi = \frac{\text{VIE} + \text{VEA}}{2} \quad (7)$$

and hardness is well-defined in the density functional theory framework as

$$\eta = \text{VIE} - \text{VEA} \quad (8)$$

The calculated values of Gibbs function show a good correlation with the energy difference (Figure 7). There are few exceptions for values that are close to zero, but this was expected, since those small values are within the limits of the calculations' accuracy at this level of theory. Accordingly, ΔE seems to be a good enough criterion for predicting the viability of ET processes. If ΔE is negative, the electron transfer mechanism is predicted to be feasible for the free radical scavenging activity of US-SWCNTs, or any other chemical species. This means that, to study the ET process between any two molecules, the only quantities that are necessary to obtain are the vertical ionization energy (VIE) and the vertical electron affinity (VEA). This represents an efficient computational strategy, especially for large-sized systems for which frequency calculations are particularly expensive. Once the VIE and VEA values are computed, it is possible to locate the molecules on the map, and according to their relative position to identify the most probable direction of the ET, i.e., which molecule will be the electron donor and which one the electron acceptor. After this definition, it is possible to calculate ΔE , for the full electron

transfer process, and to predict if the intended process is expected to be exergonic or endergonic. It is important to emphasize that this strategy has been proven to be valid only for ET reactions.

Length and Defects. The influence of the tubes' length on their capacity to accept or donate electrons has also been analyzed using the above-described strategy. (3,3) and (5,0) US-SWCNT fragments from three (0.7 nm) to eight (2.0 nm) hexagons (h) long were modeled. In addition, the influence of different point defects (Figure 2) on the electron donor and electron acceptor capabilities of nanotubes has also been investigated. The corresponding FEDAMs are available as Supporting Information (Figures 1S and 2S). According to them, the electron donor capacity of *armchair* nanotubes increases as the tubes become longer. On the contrary, for *zigzag* tubes, 4h (1 nm) was found to be the one with the highest electron donor and electron acceptor capacity. A plot of RIE and REA as a function of the length is also included as Supporting Information (Figures 3S and 4S). There is not an odd–even trend, and it can be seen that the role of the length in the antiradical capability is negligible because the differences are smaller than the differences with the electron donor capability of the free radicals. The maximum difference is 1 eV, and this variation does not modify the conclusions, since all of the US-SWCNTs have more or less the same electron donor capacity and they are on the same region of the FEDAM. The difference between the electron donor–acceptor capacity of US-SWCNTs and the electron donor–acceptor capacity of the free radical is larger than the differences related to the length of the nanotube. In a previous work of Hod and Scuseria,³⁶ the energy differences that they found as a function of the length are similar to our values. These authors reported the *effect of an electric field on the electronic properties of finite CNTs*, and it was essential for them to study their ground state characteristics in the absence of external perturbations. For that purpose, the length dependence of the highest occupied molecular orbital (HOMO)–lowest occupied molecular orbital (LUMO) gap could be one of the most important parameters. In our case, the most important information is the relative position of the US-SWCNTs on the FEDAM.

Concerning the effect of the defects, the electron donor properties are similar for the *armchair* SWCNTs with and without defects, while they are slightly higher for the *zigzag* nanotubes without defects than for those with defects. In both systems, the electron acceptor properties are different. The *armchair* and *zigzag* nanotubes with defects are systematically better electron acceptors than the equivalent defect-free nanotube (with the exception of the *zigzag* with Stone–Wale defect). However, the electron acceptor properties of the nanotubes are relevant only for scavenging $\text{O}_2^{\cdot-}$, since for all the studied free radicals the reaction mechanism is predicted to involve electron transfer from the nanotube to the free radical (path I). Therefore, for scavenging these free radicals, the electron donor capability of the nanotubes is the important property. Our results indicate that neither the length nor the defects have a significant effect on the free radical scavenger capacity of the US-SWCNTs, when reacting through the electron transfer mechanism, since the difference between the electron donor–acceptor capacity of US-SWCNTs and the electron donor–acceptor capacity of the free radical is larger than the differences related to the length or the defects of the nanotubes. However, this does not rule out that these structural features (defects) may play an important role on the US-SWCNT reactivity toward the free radical, when the reactions take place through a different mechanism.

Conclusions

Since carbon nanotubes are large arrays of conjugated double bonds, they are expected to have great electron donor–acceptor capabilities. This specific property makes them remarkably reactive toward free radicals. One possible application of the reactivity of nanotubes with free radicals is to use them as free radical scavengers. Such activity can take place through several different mechanisms. In this work, it was analyzed considering the electron transfer mechanism and using density functional theory for a wide variety of US-SWCNTs and free radicals. It was found that ultrashort *zigzag* nanotubes are better electron acceptors and also slightly better electron donors than their corresponding *armchair* partners. Pristine *zigzag* nanotubes were found to be better electron donors and worse electron acceptors than carboxylated US-SWCNTs. The electron donor capability of carboxylated *armchair* nanotubes was found to be equivalent to that of the pristine US-SWCNT, while they are better electron acceptors than the nonfunctionalized tubes. Our results indicate that neither the length nor the defects have a significant effect on the free radical scavenger capacity of the US-SWCNTs, when reacting through the electron transfer mechanism. The electron transfer reaction mechanism depends on the characteristics of the free radical and on the nature of the nanotubes. It was found to take place from the US-SWCNT toward the free radical for all modeled radicals except the $O_2^{\cdot-}$. For this particular species, the ET process is proposed to occur from the radical to the US-SWCNT.

Acknowledgment. This study was made possible due to funding from the Consejo Nacional de Ciencia y Tecnología (CONACyT), as well as resources provided by the Instituto de Investigaciones en Materiales IIM, UNAM. The work was carried out using a KanBalam supercomputer, provided by DGSCA, UNAM, and the facilities at Laboratorio de Supercomputo y Visualización en Paralelo of UAM Iztapalapa. The authors would like to acknowledge both Oralía L. Jiménez A and María Teresa Vázquez for their technical support. A.M. is grateful for financial support from DGAPA-UNAM-México.

Supporting Information Available: FEDAM in benzene for nanotubes with different lengths and helicities, FEDAM in benzene for nanotubes with different kinds of defects, RIE and REA as a function of the nanotube segment length, and computed values for ΔG and ΔE . This material is available free of charge via the Internet at <http://pubs.acs.org>.

References and Notes

- (1) Iijima, S. *Nature* **1991**, *354*, 56.
- (2) Ajayan, P. M. *Chem. Rev.* **1999**, *99*, 1787.
- (3) Yu, M. F.; Files, B. S.; Arepalli, S.; Ruoff, R. S. *Phys. Rev. Lett.* **2000**, *84*, 5552.
- (4) Hone, J.; Batlogg, B.; Benes, Z.; Johnson, A. T.; Fischer, J. E. *Science* **2000**, *289*, 1730.
- (5) Pantarotto, D.; Partidos, C. D.; Graff, R.; Hoebeker, J.; Briand, J. P.; Prato, M.; Bianco, A. *J. Am. Chem. Soc.* **2003**, *125*, 6160.
- (6) Holzinger, M.; Abraham, J.; Whelan, P.; Graupner, R.; Ley, L.; Hennrich, F.; Kappes, M.; Hirsch, A. *J. Am. Chem. Soc.* **2003**, *125*, 8566.

- (7) Peng, H.; Alemany, L. B.; Margrave, J. L.; Khabashesku, V. N. *J. Am. Chem. Soc.* **2003**, *125*, 15174.
- (8) Ying, Y.; Saini, R. K.; Liang, F.; Sadana, A. K.; Billups, W. E. *Org. Lett.* **2003**, *5*, 1471.
- (9) Kong, H.; Cao, C.; Yan, D. *J. Am. Chem. Soc.* **2004**, *126*, 412.
- (10) Liu, Y.; Yao, Z.; Adronov, A. *Macromolecules* **2005**, *38*, 1172.
- (11) Chattopadhyay, J.; Cortez, F. J.; Chakraborty, S.; Slater, N. K. H.; Billups, W. E. *Chem. Mater.* **2006**, *18*, 5864.
- (12) Yang, D.; Hu, J.; Wang, C. *Carbon* **2006**, *44*, 3161.
- (13) Engel, P. S.; Billups, W. E.; Abmayr, D. W.; Tsvaygboym, K.; Wang, R. *J. Phys. Chem. C* **2008**, *112*, 695.
- (14) Galano, A. *Nanoscale* **2010**, *2*, 373.
- (15) Watts, P. C. P.; Fearon, P. K.; Hsu, W. K.; Billingham, N. C.; Kroto, H. W.; Walton, D. R. M. *J. Mater. Chem.* **2003**, *13*, 491.
- (16) Fenoglio, I.; Tomatis, M.; Lison, D.; Muller, J.; Fonseca, A.; Nagy, J. B.; Fubini, B. *Free Radical Biol. Med.* **2006**, *40*, 1227.
- (17) Galano, A. *J. Phys. Chem. C* **2008**, *112*, 8922.
- (18) Lucente-Schultz, R. M.; Moore, V. C.; Leonard, A. D.; Price, B. K.; Kosynkin, D. V.; Lu, M.; Partha, R.; Conyers, J. L.; Tour, J. M. *J. Am. Chem. Soc.* **2009**, *131*, 3934.
- (19) Galano, A. *J. Phys. Chem. C* **2009**, *113*, 18487.
- (20) Price, B. K.; Lomeda, J. R.; Tour, J. M. *Chem. Mater.* **2009**, *21*, 3917.
- (21) Martínez, A.; Rodríguez-Gironés, M. A.; Barbosa, A.; Costas, M. *J. Phys. Chem. A* **2008**, *112*, 9037.
- (22) Frisch, M. J.; Trucks, G. W.; Schlegel, H. B.; Scuseria, G. E.; Robb, M. A.; Cheeseman, J. R.; Montgomery, J. A., Jr.; Vreven, T.; Kudin, K. N.; Burant, J. C.; Millam, J. M.; Iyengar, S. S.; Tomasi, J.; Barone, V.; Mennucci, B.; Cossi, M.; Scalmani, G.; Rega, N.; Petersson, G. A.; Nakatsuji, H.; Hada, M.; Ehara, M.; Toyota, K.; Fukuda, R.; Hasegawa, J.; Ishida, M.; Nakajima, T.; Honda, Y.; Kitao, O.; Nakai, H.; Klene, M.; Li, X.; Knox, J. E.; Hratchian, H. P.; Cross, J. B.; Bakken, V.; Adamo, C.; Jaramillo, J.; Gomperts, R.; Stratmann, R. E.; Yazayev, O.; Austin, A. J.; Cammi, R.; Pomelli, C.; Ochterski, J. W.; Ayala, P. Y.; Morokuma, K.; Voth, G. A.; Salvador, P.; Dannenberg, J. J.; Zakrzewski, V. G.; Dapprich, S.; Daniels, A. D.; Strain, M. C.; Farkas, O.; Malick, D. K.; Rabuck, A. D.; Raghavachari, K.; Foresman, J. B.; Ortiz, J. V.; Cui, Q.; Baboul, A. G.; Clifford, S.; Cioslowski, J.; Stefanov, B. B.; Liu, G.; Liashenko, A.; Piskorz, P.; Komaromi, I.; Martin, R. L.; Fox, D. J.; Keith, T.; Al-Laham, M. A.; Peng, C. Y.; Nanayakkara, A.; Challacombe, M.; Gill, P. M. W.; Johnson, B.; Chen, W.; Wong, M. W.; Gonzalez, C.; Pople, J. A. *Gaussian 03*, revision D.01; Gaussian, Inc.: Wallingford, CT, 2004.
- (23) Irikura, K. K.; Johnson, R. D., III; Kacker, R. N. *J. Phys. Chem. A* **2005**, *109*, 8430.
- (24) Francisco-Marquez, M.; Galano, A.; Martínez, A. *J. Phys. Chem. C* **2010**, *114*, 6363.
- (25) (a) Cancas, M. T.; Mennucci, B.; Tomasi, J. *J. Chem. Phys.* **1997**, *107*, 3032. (b) Mennucci, B.; Tomasi, J. *J. Chem. Phys.* **1997**, *106*, 5151. (c) Mennucci, B.; Cancas, E.; Tomasi, J. *J. Phys. Chem. B* **1997**, *101*, 10506. (d) Tomasi, J.; Mennucci, B.; Cancas, E. *THEOCHEM* **1999**, *464*, 211.
- (26) Martínez, A.; Vargas, R.; Galano, A. *J. Phys. Chem. B* **2009**, *113*, 12113.
- (27) Odom, T. W.; Huang, J.-L.; Kim, P.; Lieber, C. M. *J. Phys. Chem. B* **2000**, *104*, 2794.
- (28) Hirsch, A. *Angew. Chem., Int. Ed.* **2002**, *41*, 1853.
- (29) Liu, Q.; Ren, W.; Chen, Z.-G.; Wang, D.-W.; Liu, B.; Yu, B.; Li, F.; Cong, H.; Cheng, H.-M. *ACS Nano* **2008**, *2*, 1722.
- (30) Zheng, M.; Semke, E. D. *J. Am. Chem. Soc.* **2007**, *129*, 6084.
- (31) Joselevich, E.; Dai, H.; Liu, J.; Hata, K.; Windle, A. H. *Top. Appl. Phys.* **2008**, *111*, 101.
- (32) Dresselhaus, M. S.; Dresselhaus, G.; Jorio, A. *Annu. Rev. Mater. Res.* **2004**, *34*, 247.
- (33) Tasis, D.; Tagmatarchis, N.; Bianco, A.; Prato, M. *Chem. Rev.* **2006**, *106*, 1105.
- (34) Peng, H.; Alemany, L. B.; Margrave, J. L.; Khabashesku, V. N. *J. Am. Chem. Soc.* **2003**, *125*, 15174.
- (35) Galano, A.; Vargas, R.; Martínez, A. *Phys. Chem. Chem. Phys.* **2010**, *12*, 193.
- (36) Hod, O.; Scuseria, G. E. *ACS Nano* **2009**, *11*, 2243.